

# Transmission Line Faults Analysis Using S-transform and ANN

Chinmay Patil, Kaushal Dave, Pratik Hiralkar, Rahul Katore, Tejas Bhoiward, Vaishnavi Bhalerao

Department of Electrical Engineering

Shri Sant Gajanan Maharaj College of Engineering, Shegaon, Maharashtra

**Abstract:** The S-Transform (ST) and ANN-based fault detection & fault classification approach for overhead transmission lines are presented in this research. The PSCAD environment is used to simulate the test system. The current signals must be extracted at the network's transmitting end in order to use the suggested technique. ST processes the current signals to create intricate S-matrices. S-matrix algorithms that require only basic calculations and little computational time are used to calculate the Stockwell Fault Index (SFI). The energy of each phase is a different property that is estimated from the S-matrix. The back propagation neural network classifies the type of fault by feeding it the energy content of each phase as determined by S-matrices of various fault states. On the basis of 65 fault condition simulations, a detection and classification system based on these parameters has been created. By altering the fault inception angle (FIA), numerous fault situations have been obtained. The suggested system was written in MATLAB, and quick and precise results were produced. Future ST implementations are planned to be computationally quick.

**Keywords:** Stockwell transform, Stockwell fault index, S-matrix, Transmission line faults, ANN

## I. INTRODUCTION

An essential component of contemporary power systems are transmission lines. Any issues with them could result in an unfavorable power supply disruption. It is crucial to conduct a precise study of these problems in order to guarantee a constant flow of power. To resolve any such issues and restore the system to normal functioning, fault detection and classification are required for this purpose.

Effective transmission line protection systems have been created using mathematical and signal processing approaches. These methods make it easier to identify faults and distinguish between unhealthy and defective conditions, which makes it easier to run the relays that protect the lines. The authors of [1] have suggested a travelling wave based algorithm to identify, categorize, and locate transmission line faults on transient recovery voltage. Hybrid Signal Processing Fault Index (HSPFI), which is obtained by multiplying Stockwell Fault Index (SFI), Wigner Fault Index (WFI), and Alienation Coefficient Fault Index (ACFI) element to element, is the algorithm presented by the authors in [2] to detect and categorize transmission line failures. The authors of [3] look into how two hyper-parameters affect how well a neural network performs. It was found that, above a certain threshold, increasing the network size had no positive impact on defect detection accuracy. Back propagation neural network with 97.9% accuracy for fault classification is proposed in [4]. In [5], the current signal's S-transformation is used to calculate the S-matrix. To identify transmission line faults, the absolute median of the S-matrix is generated and given the name Stockwell Fault Index. In [6], the authors suggested an approach to choose the phase and find the defect in a triangle transmission line network using ST and ANN.

The study described in this paper focuses on providing a system for identifying and categorizing different transmission line fault types utilizing the median and energy content of each phase based on the Stockwell Transform, respectively. For fault identification, a fault index is suggested, and the energy content of each phase is sent to the back propagation neural network for fault categorization. In the proposed study, faults on transmission lines such as double line (LL), double line to ground (LLG), line to ground (LG), and three phase fault with ground involvement (LLLG) are explored.

### 1.1 Paper Outline

The research contents in the study are arranged in six sections. The background of the research and contribution is introduced in first section. Test System is described in second section. In section three, fault detection using S-transform is described. ANN and back propagation algorithm is detailed in fourth section. Fault classification based on ANN and its performance is discussed in fifth section. Research work is concluded in sixth section

### 1.2 Proposed Methodology

To detect and classify transmission line faults following methodology is proposed:

- 1) Simulate the test system under healthy and faulty conditions.
- 2) Capture the line current signals.
- 3) Transformed the captured current signal using S-transform.
- 4) Calculate absolute median of S-matrix and designate it as a Stockwell Fault Index (SFI).
- 5) Extract the feature energy from S-matrix for each phase and feed it to ANN for fault type classification.

## II. POWER SYSTEM UNDER STUDY

For the data generation purpose, a test system of 2 bus system is modelled in PSCAD environment. It is 500kV, 50Hz, three phase power system network as shown in Fig.1. The length of transmission line is 220km. The sampling frequency is 4 kHz and duration of run is 0.5sec. Following five types of fault are simulated in this system:

- LG (line to ground fault)
- LL(line to line fault)
- LLG(Double line to ground fault)
- LLL(Triple line fault)
- LLLG(Triple line to ground fault)

All the faults are initiated at the middle of transmission line i.e. at 110km from both end of transmission line. A fault resistance considered is 0.01Ω. The fault inception angles are varied from 0° to 360° in steps of 30° for each type of fault. Therefore, the total number of fault cases in this system is 13x5=65. System parameters are referred from the [2]

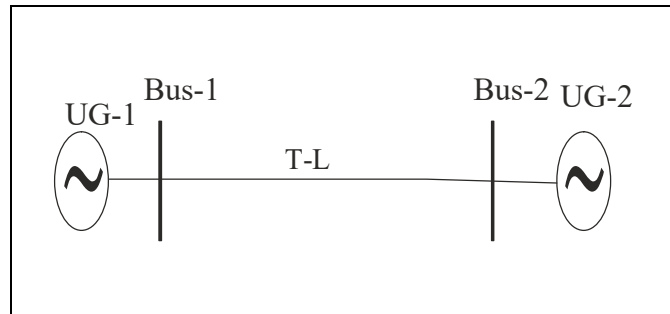


Fig-1: Single Line Diagram of 2 bus system

## III. FAULT DETECTION USING S TRANSFORM

The suggested transmission line protection technology requires the usage of a predetermined fault index for fault detection. The Stockwell transform is used to detect flaws. The fault index computation and a brief description of the Stockwell transform are discussed in further detail in the subsections that follow.

### 3.1 Feature extraction by S-transform

The S-Transform is a better variant of the continuous Wavelet Transform. The CWT,  $W(\tau, d)$  of a function  $h(t)$  is defined as

$$W(\tau, d) = \int_{-\infty}^{\infty} h(t)w(t - \tau, d)dt \quad (1)$$

where,  $W(\tau, d)$  is a scaled replica of the fundamental mother wavelet.

The dilation factor  $d$  in equation (1) is the inverse of the frequency  $f$ . The dilation influences the resolution by determining the width of the wavelet. The S-Transform is calculated by multiplying the CWT by a phase factor, which is specified below.

$$S(\tau, f) = e^{i2\pi f \tau} W(d, \tau) \quad (2)$$

where the mother wavelet for this case is defined as

$$w(t, f) = \frac{|f|}{\sqrt{2\pi}} e^{-\frac{t^2 f^2}{2}} e^{-j2\pi f t} \quad (3)$$

Thus, final form of the continuous S-transform is obtained as

$$S(\tau, f) = \int_{-\infty}^{\infty} h(t) \frac{|f|}{\sqrt{2\pi}} e^{-\frac{(\tau-t)^2 f^2}{2}} e^{-j2\pi f t} dt \quad (4)$$

and width of the Gaussian window is

$$\sigma(f) = T = 1/|f| \quad (5)$$

As a result, the S-transform is a subset of short time Fourier transformations (STFT) that employs a function with a Gaussian window. The S-transform can provide better frequency resolution for lower frequencies by employing a bigger time domain window. It can provide a higher time resolution for higher frequency by using a narrower window. The S-matrix is the S transform's output matrix. The S-matrix can be used to calculate the frequency and amplitude of a signal. [9]-[10].

#### IV. ARTIFICIAL NEURAL NETWORK (ANN)

The artificial neural network (ANN) is a computational model based on the structures and functions of biological neural networks. The components and actions of biological neural networks are the basis for the ANN computational model. The internal structure of an ANN changes in response to input and output. ANN is a nonlinear statistical data where the intricate interactions between input and output are defined.[11] ANN layers are made up of many interconnected nodes, also known as neurons. The feed forward algorithm and the back propagation technique are used in this strategy. The feed forward method moves input data from the input nodes to the output nodes via hidden nodes. In the propagation method, the input is used as a training set to generate a set of output states. Aside from that, weights are assigned to error values at random, and biases are reduced to produce the correct output [12]. In the ANN, the transfer function is employed to explain the nonlinear relationship between the input and the output [13]. Figure 2 depicts a basic Multi-layer Neural Network with three layers: input layer, hidden layer, and output layer. One or more hidden layers are interfaced with by the input layer. While neurons in the hidden layer are known as perceptron's and are linked to the output layer.

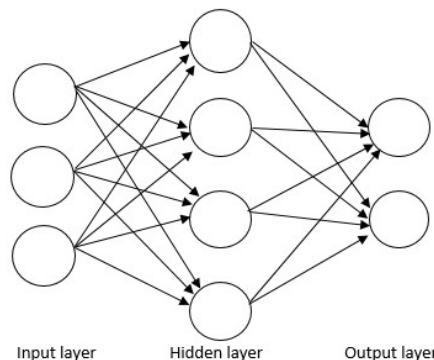


Fig. 2. The standard Multi-layer Neural Network

#### 4.1 Back Propagation Algorithm (BPNN)

Backpropagation neural network output is known as feedback to the input in order to calculate changes in weights value [14]. At each iteration and point, the error is calculated by starting from the last step and returning the considered mistake. The BPNN weights are chosen at random and fed back into an input pair before collecting the results. Following each step, the weights are updated to a new value, and the process is repeated for each set of input-output

configurations available in the creator's training data [15]. The technique is repeated until the network merges for the target values and error tolerance set. In reverse order, the full procedure is acquired for each tier of the network. Because it can train large amounts of data, BPNN is used for training [16]. Each iteration's error is calculated using the mean square approach (MSE). The following is the BPNN algorithm:

Forward propagation

$$a_j = \sum_i^m w_{ji}^1 x_i \quad (1)$$

$$z_j = f(a_j) \quad (2)$$

$$y_j = \sum_i^M w_{kj}^2 z_j \quad (3)$$

Output difference

$$\delta_k = y_k - t_k \quad (4)$$

3. Back propagation for hidden layers

$$\delta_j = (1 - z_j^2) \sum_{k=1}^K w_{kj} \delta_k$$

The MSE for each output in individual iteration is represented mathematically by

$$MSe = \frac{1}{N} \sum_1^N (E_i - E_0)^2 \quad (5)$$

Where  $a_j$  and  $w_{ji}$  are the weights of the sum of inputs and the connections.  $x_i$  and  $y_i$  represent the data for the  $i$ th input and output layer,  $z_j$  represents the activation unit of (input) connected to unit  $j$ , and  $y_k$  represents the activation output of unit  $k$ .  $\delta_k$  is the derivative of error at the  $k$ th neuron,  $\delta_j$  is the derivative of error in relation to  $a_j$ , and  $t_k$  is the input target. The model's actual output, where  $N$  is the number of iterations.

#### 4.2 ANN Design for Fault Classification

The fault classification network has three inputs and five outputs, and it was built with 200 training data sets for each. The training data consists of 65 samples for nine faults and no faults as input data. The five target output data showed LG, LL, LLG, LLL, LLLG fault states with values of 1 and 0. The Scaled Conjugate Gradient (traincsg) training technique was chosen since it required less memory and was ideal for low memory scenarios. To classify the problem in the neural network, a pattern recognition technique was applied. The energy of the three phases retrieved from the ST matrix by normalising in the frequency domain is sent into the ANN module. 75% of the data is training, whereas 25% is testing.

### V. RESULT AND DISCUSSION

#### 5.1 S-TRANSFORM BASED SIMULATION RESULTS WITH THEIR DISCUSSION

This section describes the simulation findings for detecting faults in power system lines using the proposed fault index. On the 2 Bus network, various types of faults have been created, and the current of all phases has been captured in the middle of the transmission line. After analysing 65 data sets of each defect with varied inception angles of 30 degrees, the fault threshold value is established at 0.85. The subsections that follow go over the simulation results of various faults at a 0-degree inception angle.

##### A. Phase to Ground Fault

A fault involving one phase and ground (LG) has been simulated by grounding phase-A. Figure 3 shows current waveforms in all phases during an LG failure on phase-A. The present magnitude of phase-A increases from 172 A to 800 A. The amplitude of current, however, remains constant in all healthy stages (phases A and B).

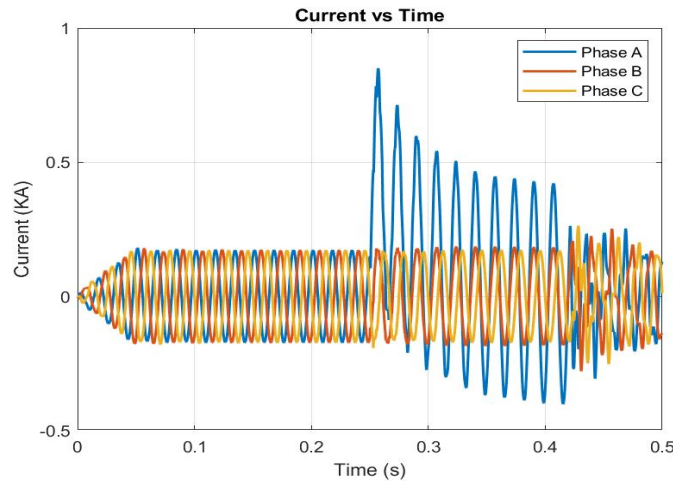


Fig. 3 Current waveforms during LG fault

The values of proposed fault index for all the three phases in the event of LG fault simulated on phase-A have been shown in Fig. 4. This is observed and identified that value of proposed fault index is higher than the threshold value (0.85 in this case) whereas the fault indices have values lower than the threshold for the healthy phases. The fault index value for the faulty phase is 0.87. Hence, the LG fault is detected effectively.

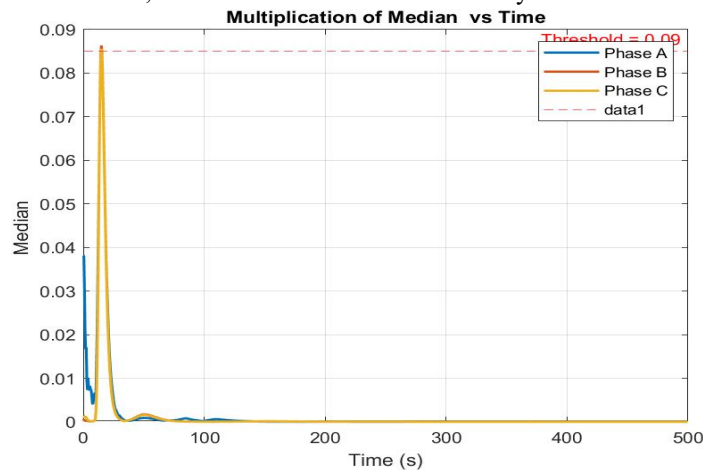


Fig. 4. Fault index calculated using current waveform during LG fault.

### B. Double Line Fault

Short circuiting phases A and B simulates a fault involving two phases without the participation of ground (LL). Figure 5 depicts three-phase current waveforms in the event of an LL failure on phases A and B. The present magnitude of phases A and B has been increased from 172 A to 1000 A, as measured and identified. However, the magnitude of current in phase-C (the healthy phase) remains the same as before the fault.

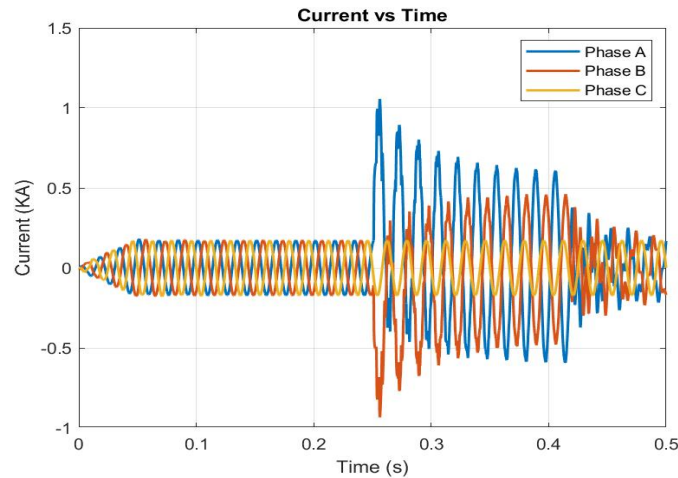


Fig. 5 Current waveforms during LL fault

Figure 6 depicts the values of projected fault indices for all three phases in the event of an LL fault affecting phases A&B. It has been seen and determined that the fault indices for the faulty phases A and B are more than the threshold value of 0.872. The fault index for the healthy phase (phase C) is 0.85, which is less than the threshold value. As a result, the suggested technique effectively detects the LL failure.

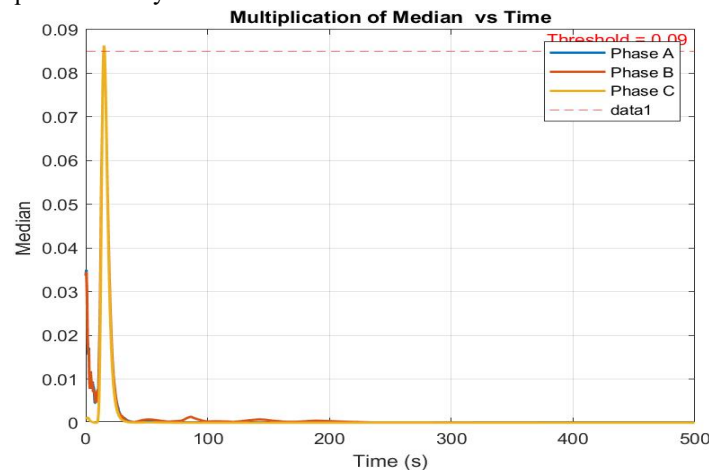


Fig. 6. Fault index calculated using current waveform during LL fault.

### C. Double Line to Ground Fault

By concurrently grounding phases A and B, the fault involving two phases and ground (LLG) has been simulated. In the case of an LLG fault, the current waveforms for all three phases are depicted in Fig.7. The magnitude of current in phases A and B has been increased from 172 A to 1200 A. However, the magnitude of current in phase-C (healthy phase) remains unchanged from before the fault.

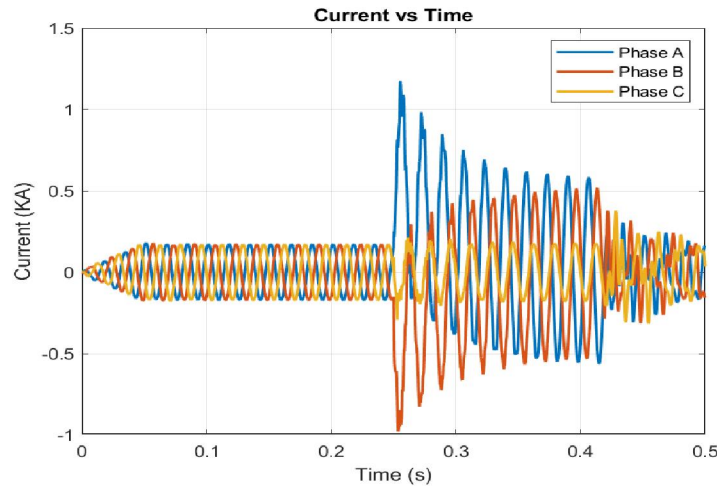


Fig. 7 Current waveforms during LLG fault

Figure 8 depicts the suggested fault index values for all three phases in the event of an LLG fault involving phases A&B. This is recognised and observed that the values of fault indices corresponding to faulty phases A and B are more than the threshold value of 0.85. The fault index for the healthy phase (phase-C) is 0.874, which is less than the cutoff value. As a result, the suggested technique effectively detects the LLG defect.

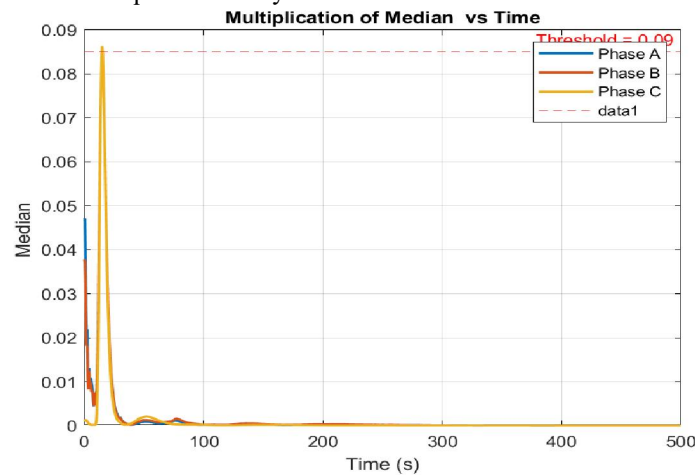


Fig. 8. Fault index calculated using current waveform during LLG fault.

#### D. Three Phase Fault Involving Ground

To replicate the three phase to ground fault (LLG), all three phases are simultaneously grounded. Figure 9 depicts three phase current waveforms during the fault period. The present magnitude of all three phases has increased from 172 A to 1350 A, as measured and predicted. However, the magnitude of current in phase-C (healthy phase) remains unchanged from before the fault.

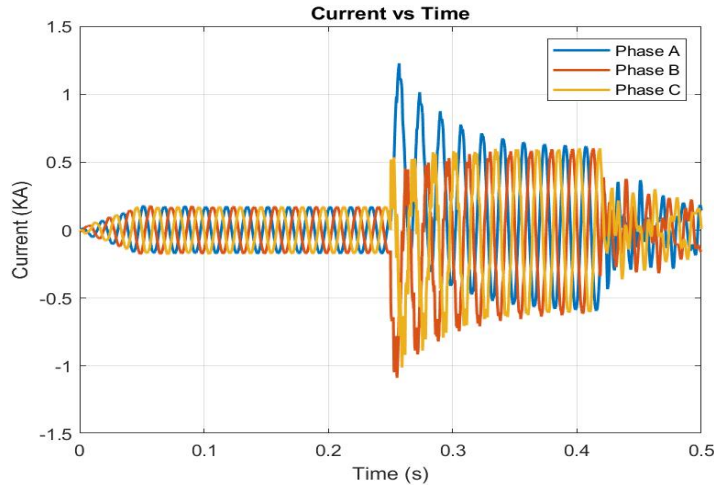


Fig. 9 Current waveforms during LLLG fault

The values of proposed fault index for all the three phases during the LLLG fault have been shown in Fig.10. This is observed predicted that values of fault indices of all phases are higher compared to the threshold value and also above . Hence, the LLLG fault is effectively detected using the proposed algorithm.

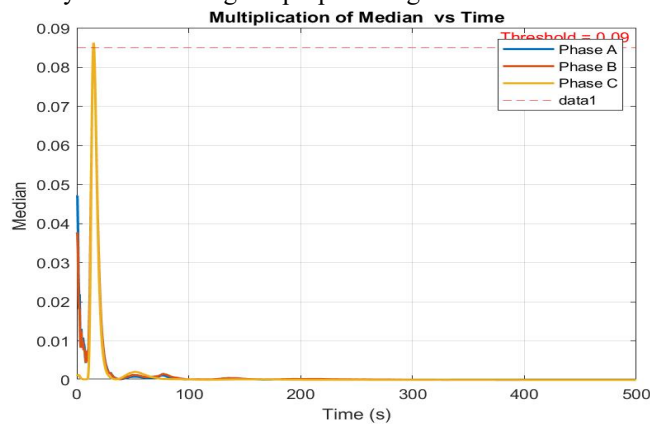


Fig. 10. Fault index calculated using current waveform during LG fault.

**E. Three Phase Line Fault**

Without the ground (LLL), all three phases are replicated at the same time. Figure 11 depicts three phase current waveforms during the fault period. The present magnitude of all three phases has increased from 172 A to 1300 A, as measured and predicted.

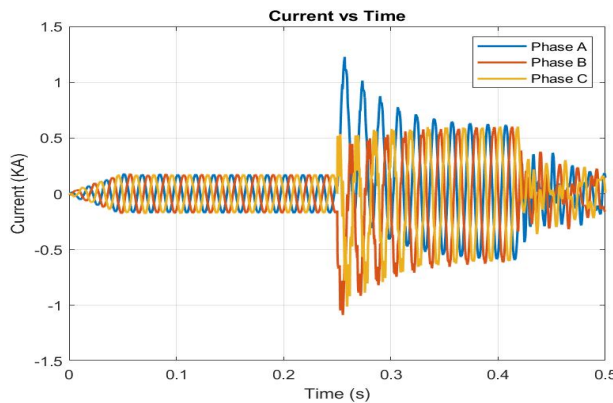


Fig. 11 Current waveforms during LLL fault

Figure 12 depicts the suggested fault index values for all three phases during the LLL fault. This is predicted by the fact that the values of fault indices for all phases are more than or equal to the threshold value. As a result, the suggested technique effectively detects the LLL error.

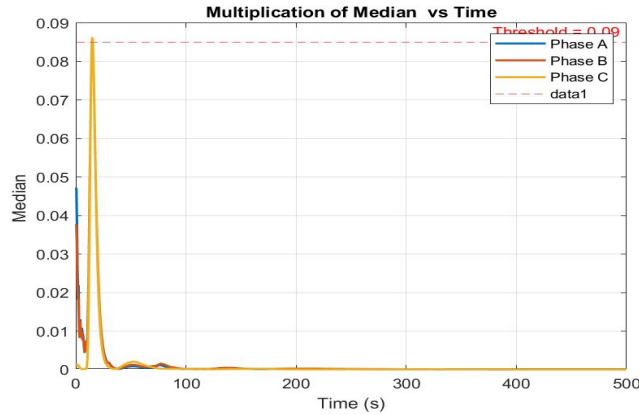


Fig. 12. Fault index calculated using current waveform during LG fault.

### 5.2 ANN BASED SIMULATION RESULTS WITH THEIR DISCUSSION

The configuration 3-10-5 was chosen as the best ANN fault classification performance. There are four types of confusion matrices: training, validation, testing, and overall.

Output Class	LG fault	LL	LLG	LLL	LLLG	Percentage
LG fault	8 25.0%	0 0.0%	0 0.0%	0 0.0%	0 0.0%	100% 0.0%
LL	0 0.0%	6 18.8%	0 0.0%	0 0.0%	0 0.0%	100% 0.0%
LLG	0 0.0%	0 0.0%	7 21.9%	0 0.0%	0 0.0%	100% 0.0%
LLL	0 0.0%	0 0.0%	0 0.0%	5 15.6%	0 0.0%	100% 0.0%
LLLG	0 0.0%	0 0.0%	0 0.0%	0 0.0%	6 18.8%	100% 0.0%
Percentage	100% 0.0%	100% 0.0%	100% 0.0%	100% 0.0%	100% 0.0%	100% 0.0%

Fig.13. Training confusion matrix.

Output Class	LG fault	LL	LLG	LLL	LLLG	Percentage
LG fault	5 15.2%	0 0.0%	0 0.0%	0 0.0%	0 0.0%	100% 0.0%
LL	0 0.0%	8 24.2%	0 0.0%	0 0.0%	1 3.0%	88.9% 11.1%
LLG	0 0.0%	1 3.0%	5 15.2%	0 0.0%	0 0.0%	83.3% 16.7%
LLL	0 0.0%	0 0.0%	0 0.0%	6 18.2%	2 6.1%	75.0% 25.0%
LLLG	0 0.0%	0 0.0%	0 0.0%	1 3.0%	4 12.1%	80.0% 20.0%
Percentage	100% 0.0%	88.9% 11.1%	100% 0.0%	85.7% 14.3%	57.1% 42.9%	84.8% 15.2%

Fig . 14. Testing confusion matrix.

**Validation Confusion Matrix**

Output Class	LG fault	5 22.7%	0 0.0%	0 0.0%	0 0.0%	0 0.0%	100% 0.0%
	LL	0 0.0%	4 18.2%	0 0.0%	0 0.0%	0 0.0%	100% 0.0%
	LLG	0 0.0%	1 4.5%	3 13.6%	0 0.0%	0 0.0%	75.0% 25.0%
	LLL	0 0.0%	0 0.0%	1 4.5%	7 31.8%	1 4.5%	77.8% 22.2%
	LLLG	0 0.0%	0 0.0%	0 0.0%	0 0.0%	0 0.0%	NaN% NaN%
	Percentage	100% 0.0%	80.0% 20.0%	75.0% 25.0%	100% 0.0%	0.0% 100%	86.4% 13.6%
		LG fault	LL	LLG	LLL	LLLG	Percentage
		Target Class					

Fig.15.Validation confusion matrix.

**Overall Confusion Matrix**

Output Class	LG fault	13 20.0%	0 0.0%	0 0.0%	0 0.0%	0 0.0%	100% 0.0%
	LL	0 0.0%	12 18.5%	0 0.0%	0 0.0%	0 0.0%	100% 0.0%
	LLG	0 0.0%	1 1.5%	13 20.0%	0 0.0%	1 1.5%	86.7% 13.3%
	LLL	0 0.0%	0 0.0%	0 0.0%	11 16.9%	0 0.0%	100% 0.0%
	LLLG	0 0.0%	0 0.0%	0 0.0%	2 3.1%	12 18.5%	85.7% 14.3%
	Percentage	100% 0.0%	92.3% 7.7%	100% 0.0%	84.6% 15.4%	92.3% 7.7%	93.8% 6.2%
		LG fault	LL	LLG	LLL	LLLG	Percentage
		Target Class					

Fig 16. Overall confusion matrix.

Figure 13 depicts a training confusion matrix graphic. Whereas 75% of the data is used for training, the matrix has a 100% efficiency. Figures 14 and 15 show the testing and validation confusion matrix plotted with efficiencies of 84.8% and 86.4%, respectively. Figure 16 depicts the overall confusion matrix, with 93.8% properly classifying the defect in the dark grey box and 6.2% incorrectly classifying the fault. The green box represents the number of fault types that have been correctly classified, whereas the red box represents the number of fault types that have been incorrectly classified. [17] Overall, the fault categorization results show a satisfactory performance.

## VI. CONCLUSION

This paper proposes a transmission line protection strategy based on the Stockwell Transform. The proposed investigation is carried out in MATLAB/Simulink utilising a two-bus test system. A fault index has been proposed to detect various defects in power system networks such as LG, LL, LLG, and LLLG. The fault index has been successfully used for detecting problematic phases and separating them from healthy phases.

The use of ANN for fault classification of transmission line faults with energy as the extracted feature was thoroughly investigated. The study found that ANN performs well in classifying faults when trained using validated training data. As input values, the network utilised three phase energy. Changing the size of the training data set, the number of hidden layers, and the number of neurons in each layer can all enhance performance.

**REFERENCES**

- [1] Rafael Arranz , Angel Paredes, Francisco Munoz,” Fault location in Transmission System based on Transient Recovery Voltage using Stockwell transform and Artificial Neural Networks”, Electrical power research, 2021,pp.1-12
- [2] Anup Kumar,Himanshu Sharma,Ram Niwash Mahia,Om Prakash Mahela and Baseem Khan,” Design and Implementation of Hybrid Transmission Line Protection Scheme Using Signal Processing Techniques”, Hindawi,2022
- [3] Seongmin Heo and Jay H. Lee, “Fault detection and classification using artificial neural networks”, IFAC Conference, Elsevier, 2018, pp.470-475
- [4] Santosh K. Padhy, Basanta K.Panigrahi, Prakash K. Ray et.al “CLASSIFICATION OF FAULTS IN A TRANSMISSION LINE USING ARTIFICIAL NEURAL NETWORK” , International Conference on Information Technology,2018
- [5] Sheesh Ram Ola, Amit Saraswat , Sunil Kumar Goyal, S. K. Jhajharia, Om Prakash Mahela ,”A Technique Using Stockwell Transform Based Median for Detection of Power System Faults”,IEEE,2018
- [6]H. Shu, Q. Wu, X. Wang, X. Tian, “Fault phase selection and distance location based on ANN and s-transform for transmission line in triangle network” Proceedings of the 3rd International Congress on Image and Signal Processing volume 7, 2010, pp. 3217–3219
- [7]Mohammad Javad Dehghani ,” Comparison of S-transform and Wavelet Transform in Power Quality Analysis”,World Academy of Science, Engineering and Technology International Journal of Electrical and Computer Engineering Vol.3,2009, pp.225-228
- [8] Eisa Bashier, M. Tayeb Orner ,AI Aziz AlRhir “Transmission Line Faults Detection, Classification and Location using Artificial Neural Network” , IEEE,2012
- [9] Zahra Moravej, Mohammad Pazoki, and Mojtaba Khederzadeh, “New Pattern-Recognition Method for Fault Analysis in Transmission Line With UPFC,” IEEE Transactions on Power Delivery, Vol. 30, No. 3, June 2015, pp. 1231-1242.
- [10] Flavio B. Costa, “Fault-Induced Transient Detection Based on Real-Time Analysis of the Wavelet Coefficient Energy,” IEEE Transactions on Power Delivery, Vol. 29, No. 1, February 2014, pp. 140-153.
- [11] K. Chen, C. Huang, and J. He, “Fault detection, classification and location for transmission lines and distribution systems: a review on the methods,” High Volt., vol. 1, no. 1, pp. 25–33, 2016.
- [12] J. Holkar and P. V. Fulmali, “Fault Analysis on Transmission Lines using Artificial Neural Network,” IJESRT, vol. 5, no. 2, pp. 863– 871, 2016.
- [13] S. K. Kumar, M. SwamyR, and V. Venkatesh, “Artificial Neural Network Based Method for Location and Classification of Faults on a Transmission Lines,” International Journal of Scientific Research & Publication, vol. 4, no. 1, pp. 2250–3153, 2014.
- [14] M. Jamil, S. K. Sharma, and R. Singh, “Fault detection and classification in electrical power transmission system using artificial neural network,” Springerplus, vol. 4, no. 1, 2015.
- [15] S. Upadhyay, S. R. Kapoor, and R. Choudhary, “Fault Classification and Detection in Transmission Lines using ANN”, International Conference on Inventive Research in Computing Application (ICIRCA), 2018,pp. 1029–1034.
- [16] M. Technologiae, “The Application of Artificial Neural Networks to Transmission Line Fault Detection and Diagnosis,” University of South Africa, 2016.
- [17] S. B. Ayyagari, “ARTIFICIAL NEURAL NETWORK BASED FAULT LOCATION FOR,” University of Kentucky Master’s Thesis,2011.